18th International Conference on Structural Mechanics in Reactor Technology (SMiRT 18)
Beijing, China, August 7-12, 2005
SMiRT18- G10-3

DHC BEHAVIOUR OF IRRADIATED ZR-2.5NB PRESSURE TUBES UP TO 365^{O}C

M. Resta Levi
Atomic Energy of Canada Limited
Chalk River Laboratories
Chalk River, Ontario, Canada, K0J 1J0
Phone: 613-584-8811+4206
Fax: 613-584-8214
E-mail: restalevim@aecl.ca

M.P. Puls
Atomic Energy of Canada Limited
2251 Speakman Drive,
Mississauga,Ontario,Canada L5K 1B2
Phone: 905-823-9060+3279,
Fax: 905-403-7385
E-mail: pulsm@aecl.ca

ABSTRACT

Under certain conditions, zirconium alloy pressure tubes in CANDU® reactors can be susceptible to a mechanism of cracking called Delayed Hydride Cracking (DHC). The rate of initial crack penetration and propagation is typically low, and permits sufficient time for leak detection before an unstable crack length is obtained, termed Leak-Before-Break. Since the DHC velocity is temperature dependent, it is necessary to quantify the DHC velocity over the range of operating temperatures in order to confirm that the margins against unstable fracture are adequate to ensure Leak-Before-Break. The objective of the present work is to establish the DHC temperature dependence in irradiated material to a higher temperature than has been done previously. The results from an ex-service (irradiated) cold-worked Zr-2.5Nb pressure tube doped to a hydrogen isotope concentration of 153 wt ppm shows that between 150 and 325^{o}C the DHC velocity follows an Arrhenius relationship. At temperatures higher than 325^{o}C, the velocity deviates from the Arrhenius relationship, proceeding at much lower velocities until an upper temperature limit for DHC is achieved at about 365^{o}C. The physical reason for the observed cessation temperature for DHC in this material, containing only 153 wt ppm hydrogen isotope, is thought to be due to insufficient hydrogen, making hydride nucleation at the crack tip impossible. It is expected that the strength-based DHC cessation temperature in irradiated material containing sufficient hydrogen would be higher.

Keywords: CANDU pressure tubes, Zr-2.5%Nb alloy, Delayed Hydride Cracking, Leak Before Break.

1. INTRODUCTION

CANDU Pressurized Heavy Water Reactors (PHWR) contain pressure tubes made of a cold-worked Zr-2.5Nb alloy. The pressure tubes, which contain the fuel, are pressurized with hot heavy water and serve as the primary pressure boundary for the heat transport system within the reactor core. During service the pressure tubes absorb deuterium from the environment. If a sufficient amount of deuterium were absorbed at a defect region, the Zr-2.5Nb alloy may become susceptible to a cracking mechanism known as Delayed Hydride Cracking (DHC). The industry developed safeguards to prevent crack initiation by DHC. The safeguards consist of periodic inspections of the pressure tubes and of methodologies used for assessing flaws that may be detected as a result of inspections. In addition, as defence in depth, a Leak-Before-Break methodology is used [1]. This methodology enables the reactor operators to detect a leaking crack and shut the reactor down, stopping crack growth before the crack reaches a critical size. One of the important parameters used in Leak-Before-Break analysis is the rate of growth (or crack velocity) of a growing DHC crack in the axial direction with respect to the pressure tube geometry. Since the DHC velocity is temperature dependent, it is necessary to measure it over the range of operating temperatures in order to confirm that the margins against unstable fracture are adequate to ensure Leak-Before-Break. The DHC process is thermally activated and the crack velocity follows an Arrhenius

® Registered Trade Mark of Atomic Energy of Canada Ltd.

relationship. A database of crack velocities has been obtained on ex-service pressure tubes, which were removed from CANDU reactors for various reasons [2]. The database is relevant to the operating temperatures for CANDU reactors. However, because future CANDU reactors may operate at higher temperatures, it is necessary to determine if the crack velocity would continue to increase following this Arrhenius relationship, or if it would decrease with increasing temperature and eventually become zero when a "limit" temperature is reached. A previous study presented the results for unirradiated material and included a limited study on irradiated material [3]. The objective of the present work is to establish the DHC threshold stress intensity factor and velocity temperature dependence in irradiated material having a higher hydrogen concentration than in the previous case, compare the results with previous ones from unirradiated pressure tube material and model the behaviour.

2. EXPERIMENTAL

2.1 Materials and Specimens

The DHC velocity properties were measured on a section from the outlet end of irradiated cold-worked Zr-2.5Nb pressure tube material. The in-service irradiation temperature and neutron fluence at the outlet section were about 292°C and 3.5 x10^{25} n/m^2, E > 1 MeV, respectively.

The material was doped with hydrogen to about 153 wt ppm [H_{eq}][1] by electrolytically depositing a hydride layer on the surface of the tube sections and then anneal-diffusing hydrogen into the matrix. The material was first annealed for 96 h at 300°C to dissolve the hydride layer into the matrix and then re-hydrided and re-homogenized at 386°C for 29 h. This annealing probably recovered irradiation damage to some extent that we estimate to result in a 10% reduction in the yield strength of the materials tested.

DHC testing in the axial and radial directions with respect to the pressure tube geometry were performed on Curved Compact Toughness (CCT) and Cantilever Beam (CB) specimens, respectively (Figs 1 through 3).

2.2 DHC Velocity Tests

A schematic diagram of the test apparatus is shown in Fig. 4. DHC velocity was measured on pre-fatigued CCT specimens (Fig. 1). The specimens were initially heated to 386°C and then cooled to different test temperatures. Once the test temperature was attained, the specimens were loaded. The load was applied by a stepping motor controlled by a computer, and was monitored by a load cell. Crack growth by DHC was monitored by Acoustic Emission (AE). Tests were performed at a constant load and therefore K_I increased during testing. The initial and final K_I values are given in Table 1. Three tests at different temperatures were usually performed on a single specimen.

After testing, the specimens were broken open and the crack areas measured and the average crack depth calculated by dividing the crack area by the specimen breadth. The average crack velocity was calculated by dividing the average crack depth by the time for cracking, excluding the incubation time (the time between the load application and the onset of cracking). An example of a specimen broken open after testing is shown in Fig. 5. The figure shows different crack zones starting on the right with the pre-fatigue crack and continuing to the left with the DHC cracks obtained at different test temperatures. The last zone on the left corresponds to fast fracture resulting from the specimen being pulled apart to reveal the crack surface.

The DHC crack zones from each specimen presented different striations spacing for each test temperature. The average striation spacing in the cracking direction was measured by an interception method, which consists of dividing the length of a line-segment in the cracking direction by the number of intersections with the striations minus one.

2.3 K_{IH} Tests

K_{IH} was measured in the radial direction between 150 and 340°C using CB specimens (Fig. 2), following a load-reducing method. A schematic diagram of the test apparatus is shown in Fig. 6. Load was applied by a stepping motor with a screw drive, controlled by a computer, and was monitored by a load cell. Crack growth by DHC was monitored by AE. Specimens were initially heated to 386°C and then cooled to different test temperatures. Once the test temperature was attained, the specimen was loaded to an initial K_I of 15 to 22 MPa$\sqrt{m}$ and then the K_I was reduced in small steps (usually 2%) every time the crack progressed by DHC by a small amount (usually 5 μm). The test was stopped when the load reached a minimum were there was an absence of AE activity for at least 24 h.

[1] Total hydrogen equivalent concentration. H_{eq} = protium + 0.5 deuterium, concentrations by weight fraction

3. RESULTS

The axial crack velocities measured in the irradiated material are given in Table 1 and plotted in Fig. 7. This figure also shows the axial crack velocity of an unirradiated tube [3] and generally bounds for irradiated material of the extant axial crack velocity database [2].

The DHC velocity of the ex-service pressure tube follows an Arrhenius relationship between 150 and 325°C. At temperatures higher than 325°C, the velocity deviates from the Arrhenius relationship decreasing from 8.8×10^{-7} m/s at 325°C to 1.0×10^{-9} m/s at 360°C. A practical upper temperature limit for DHC is reached at about 365°C where the DHC velocity is very low, 3.39×10^{-11} m/s (Fig. 7). Striation spacing measurements are given in Table 1 and plotted in Fig. 8. The striation spacing has little dependence with temperature at low temperatures but rapidly increases with increasing temperature above 320°C. Table 1 also provides calculated values for this material of average plastic zone, critical hydride fracture length (L_c) and K_{IH}, using the Shi and Puls expressions [4,5].

K_{IH} results are plotted in Fig. 9. They have little dependence with temperature at low temperatures but rapidly increase with increasing temperature above 300°C. Table 2 summarizes the measured K_{IH} values and compares them with calculated values for this material, using the Shi and Puls expressions [4]. Fig. 10 and 11 show the hydride distribution and striation spacing, respectively, in a sample tested at 360°C, which is close to DHC cessation temperature.

4. DISCUSSION

In this section an attempt is made to explain what caused the DHC velocity to decrease to negligible values at 365°C, the striation spacing to increase strongly with increasing temperature above 320°C and K_{IH} to similarly increase with increasing temperature above 300°C.

4.1 K_{IH} Model

Hydride precipitation at the crack tip is a necessary condition for DHC to occur, but is not a sufficient condition. Shi and Puls [4] have postulated that a sufficient condition for DHC is for the local stress in the hydride to be greater than or equal to a threshold tensile stress for hydride fracture. Based on this criterion, expressions were derived for the critical hydride length, L_c, for fracture and K_{IH}, the threshold stress intensity factor for DHC initiation. In the subsequent assessment of the experimental results, and based on references [6,7] it is assumed that the striation spacing is a direct indicator of critical hydride length. The relations derived by Shi and Puls [4], based on various simplifying assumptions about the net stresses on the hydride and its shape as it grows, show that these parameters depend on the hydride fracture strength and the maximum applied stress (in the absence of hydride) achievable on the crack tip hydride, the latter depending on the yield strength of the matrix. These two strengths decrease in magnitude with increasing temperature, with the greatest decrease being that of the yield strength. In subsequent papers, Shi and Puls [8,5] derived expressions for the limiting conditions for DHC based on conditions for hydride nucleation and maximum hydride length. (Not considered in these studies was the effect of stress relaxation through creep, which is also able to lower the maximum applied stress acting on the hydride near the crack tip.)

4.2 Factors Controlling DHC Initiation at a Crack

The controlling factors on the temperature for hydride nucleation are the yield strength of the matrix, the amount of stress elevation above the yield strength and the amount of hydrogen concentration in solution. Temperature controls hydride fracture because of the temperature dependence of the net stress in the hydride, which must be tensile and exceed its fracture strength. The net stress in the hydride depends on temperature, since the yield strength decreases as the temperature increases. Over a certain temperature range, the net stress in the hydride can also depend on the hydrogen isotope concentration in solution, since insufficient hydrogen isotope in solution limits the hydride length. The greater the hydride length, the lower is the compressive stress in the hydride due its misfit strains alone and the less externally applied stress is needed to exceed the fracture stress of the hydride. In the following, the relations derived by Shi and Puls [4,8,5] to predict DHC cessation temperatures and K_{IH} are used to determine whether these relations could be used to rationalize the DHC cessation results of the irradiated pressure tube material.

4.3 Limiting Conditions for DHC in Unirradiated Material

Sagat and Puls [3] showed that the DHC velocity in an unirradiated pressure tube material having a total hydrogen isotope content of 170 wt ppm becomes negligible at 350°C. These results are reproduced here in Fig. 7. To explain these results, Sagat and Puls postulated that cessation of DHC was due to insufficient net tensile stress to fracture the crack tip hydrides, rather than insufficient hydrogen isotope in solution for hydrides to form at the

crack tip and to grow to a critical length. Based on the K_{IH} model of Shi and Puls [4], it was shown that K_{IH} would become infinite when the plane strain crack tip normal stress is reduced to $1.46 \cdot \sigma_y$. For the K_I values that could sensibly be applied to maintain plane strain conditions, it was suggested that DHC actually stopped when K_{IH} increased to 17 MPa$\sqrt{m}$, which implied, on the basis of the K_{IH} model, that the crack tip normal stress would have been reduced to $1.59 \cdot \sigma_y$. (In [4] the value was erroneously given as $1.52 \cdot \sigma_y$.) Not actually verified by Sagat and Puls [3] was whether, with this reduction in stress elevation at the crack tip, the hydrogen content in the material was sufficient so that hydrides could nucleate at the crack tip at 350°C. Using equation 24 of Shi et al. [5], an upper bound temperature, T_c, for hydride nucleation at a given total hydrogen content in the material can be calculated. Assuming that the three principal crack tip stresses at 350°C would be reduced by stress relaxation by the same amount from their room temperature Hutchinson-Rice-Rosengren values [9] as would need to be the reduction in the crack tip normal stress (from $3.35 \cdot \sigma_y$ to $1.59 \cdot \sigma_y$ for the latter) to increase K_{IH} to the applied K_I value, a maximum hydrostatic stress in the plastic zone of $1.239 \cdot \sigma_y$ is obtained. With this value of the hydrostatic stress and the Terminal Solid Solubility limit for hydride Precipitation (TSSP) relation for hydride nucleation from Pan et al TSSP1 [10], hydride could nucleate and grow from 371°C and lower, i.e., above the temperature of 350°C at which DHC cessation was observed. The nucleated hydride would be able to grow up to the length of the plastic zone length on the crack plane on the basis of this model because it was assumed for simplicity in deriving a simple analytic expression for T_c that the plastic zone stresses are constant from the crack tip to the plastic zone boundary. This reconfirms that in the unirradiated material containing 170 wt ppm hydrogen the strength-based, not the hydrogen-based, limit on DHC had been attained.

4.4 Limiting Conditions for DHC for Irradiated Material

To determine whether the same conclusion is true for the present results on irradiated pressure tube material containing 153 wt ppm [H_{eq}], we assume that at 365°C, where cessation of DHC was observed experimentally, the crack tip normal stress would be reduced to the same level ($1.59 \cdot \sigma_y$) as for the unirradiated material. (Experimental data (private communication with N. Badie AECL, Mississauga, Ontario, Canada, 2005) suggests that thermal creep in irradiated material is considerably suppressed. However this suppression is compensated by the strong stress dependence of the creep rate and the increase in the absolute value of the stress arising from the higher yield strength in the irradiated material.) Using the approximation for the temperature limit due to hydrogen concentration given by equation 24 from Shi at al [5], again with a plastic zone hydrostatic stress of $1.239 \cdot \sigma_y$, a measured yield strength reduced by an assumed 10% (to account for some annealing of irradiation damage) given by 900 – 1.0957·T(°C) MPa and the same TSSP1, yields 363°C, which is very close to the cessation temperature actually observed. This result suggests that for this irradiated material, cessation of DHC was due to lack of hydrogen, not due to lack of sufficient applied normal tensile stress to fracture a crack tip hydride (i.e., the strength-based limit). It should be noted that the model of Shi and Puls for K_{IH} [4] does not strictly apply when hydrides form in a broad cluster at the crack tip as shown in Fig. 10. However, qualitatively, the effect of these hydrides above and below the crack plane on the net stress acting on the hydride on the crack plane would be the same as that obtained by postulating that the applied stress acting on a single, slender hydride on the crack plane had reduced due to stress relaxation and could be a contributing factor limiting DHC when conditions are such that they result in these types of hydride distributions at the crack tip.

4.5 Theoretical Estimates of Critical Hydride Length and K_{IH}

A theoretical estimate of what might be the strength-based temperature limit for this material is difficult without experimental results for irradiated material containing more than 153 wt ppm [H_{eq}] since we see from the indirect evidence of the results of the data that the crack tip normal stress decreases both due to the reduction in the yield strength with increasing temperature and due to reduction of the plane strain stress elevation due to stress relaxation caused by thermal creep. Comparison of the striation spacing, which we assume is identical to the critical hydride length for fracture, L_c, with the plastic zone length, shows that L_c is shorter than the plastic zone length. In this case the analytical expressions given by Shi and Puls [4,8] are valid. Table 1 summarizes the results of theoretical estimates of these parameters with temperature assuming that the stress relaxation of the crack tip normal stress follows the temperature dependence of Poisson's ratio ($\nu = 0.436\text{-}4.8\times10^{-4}T(^oC)$) using for the normal stress the expression $\sigma_y/(1\text{-}2\nu)$ multiplied by 0.738 to yield $1.59 \cdot \sigma_y$ at 365°C. The calculation shows that there is a gradual increase in L_c and a slightly slower increase in K_{IH} over the entire temperature range up to DHC cessation, whereas the experiments show little temperature dependence up to 320°C for L_c and 300°C for K_{IH} after which there is a more rapid increase. One reason for the more rapid increase in these two parameters within 45 and 65°C, respectively, of the DHC cessation temperature could be the effect on these parameters of the amount of hydrogen in solution, which would prevent hydride growth at the crack tip to its critical value, if insufficient.

Using a numerical approach, Shi and Puls [8] estimated the effect. However, their simplified theoretical treatment assumes that, as K_I approaches K_{IH}, the critical hydride length would need to be longer than the plastic zone length, which is contrary to the experimental observations. In their simplified theoretical treatment, in which the crack plane normal stress in the plastic zone has a constant value with distance from the crack tip to the plastic zone boundary, once a hydride is able to nucleate it is able to grow to at least the plastic zone boundary. In reality, the plastic zone normal stress is a maximum at approximately twice the crack tip opening displacement and then decreases slowly with distance from there. Therefore, even when L_c remains within the plastic zone, because of the decrease of the normal and hydrostatic stresses with distance from the crack tip within this zone, the peak of which depends on K_I [9], the maximum diffusion-limited hydride length would be sensitive to the applied K_I and would increase as the applied K_I approaches K_{IH} because this parameter is increasing rapidly with temperature due to the rapid decrease of hydrogen in solution with temperature.

4.6 Limiting DHC Velocity Behaviour of Unirradiated and Irradiated Material

To obtain the maximum possible crack velocity at a given temperature, the specimens must be cooled from above the Terminal Solid Solubility limit for hydride Dissolution (TSSD) [10] to a temperature above the Terminal Solid Solubility limit for hydride Precipitation (TSSP) [10]. This ensures that the matrix contains the maximum possible concentration of hydrogen [11]. When the temperature is lowered so that the hydrogen concentration in solution is given everywhere by the TSSP boundary, hydride can grow anywhere in the solid, and the maximum possible concentration in solution able to diffuse to the crack tip at that temperature is obtained. Above that temperature, the concentration in solution far from the crack is insufficient to precipitate hydride there and the amount of hydrogen available for diffusion to the crack tip would be less than the maximum amount possible if the material had had a higher hydrogen content. This causes the rate of diffusion, and hence the growth rate of the crack-tip hydride to its critical length, to decrease rapidly with increase in temperature. This provides the explanation for the rapid decrease in DHC velocity of the irradiated material with 153 wt ppm [H_{eq}]. The explanation for the reduction in DHC velocity in unirradiated material prior to reaching the hydride fracture limit is that the critical hydride length becomes very large and is growing well outside the plastic zone, resulting in a rapidly reducing concentration gradient as the fracture limit is approached.

As expected, the DHC velocity in the irradiated material is higher than that of the unirradiated material (Fig. 7) [2, 3]. In addition, the temperature at which the DHC velocity starts to deviate from the Arrhenius relationship is about 15°C higher in the irradiated compared to the unirradiated material (325 and 310°C, respectively). A similar shift in temperature is observed in the upper temperature limit for DHC (365 and 350°C, respectively). However, as discussed in the foregoing, if the irradiated material would have contained more hydrogen, it would be expected that the deviation from the Arrhenius relationship and the DHC cessation temperature would be somewhat higher. An accurate estimate of this temperature is difficult to determine as it depends on knowledge of the temperature dependence of the yield and hydride fracture strengths and the amount of stress relaxation in material under irradiation at elevated temperatures.

5. CONCLUSIONS

The present study was carried out because future CANDU reactors, such as the Advanced CANDU Reactor™ (ACR), may operate at higher temperatures than the current ones. For analysis of Leak-Before-Break, linear extrapolation of the Arrhenius dependence of the axial DHC velocity data could lead to overly conservative estimates of DHC velocities at outlet operating temperatures if there were a decrease in the DHC velocity with increasing temperature due to reasons other than lack of sufficient hydrogen. The techniques presently available to hydride irradiated pressure tube material, while largely retaining their irradiation-induced mechanical properties, limited the total doping of hydrogen isotope of the samples to 153 wt ppm. The results of tests on this irradiated pressure tube material are that the DHC velocity follows the previously obtained Arrhenius temperature dependence to at least 325°C.

The decrease in DHC velocity above 325°C to negligible values at 365°C is analysed to be due to insufficient hydrogen isotope for hydride nucleation at the crack tip in this irradiated material. It is estimated that if the material had contained a higher concentration of hydrogen isotope the hydride-fracture-based limit to DHC would be higher than 365°C. A reliable theoretical estimate of this limit is difficult to make with our current knowledge since it depends on extrapolating the temperature dependence of the yield strength, hydride fracture strength and crack-tip stress relaxation of irradiated material to temperatures where there might be significant increases in their temperature sensitivities. To determine this hydride-fracture-based limit for DHC in irradiated material would also require methods of hydrogen isotope doping that can produce higher concentrations than achievable with the present technique without removing the irradiation-induced strengthening of the material. In addition, irradiation

of the pressure tube material at higher temperatures is necessary to ensure representative values are obtained for the irradiation-induced mechanical and microstructural properties that govern DHC.

Determining at what temperature beyond 325°C is the hydride fracture-based limit to DHC in irradiated pressure tube material is really only of concern in the unlikely event that a pressure tube were to exceed 100 wt ppm and, in addition, were operated so that its pressure tube outlet temperature were approached from well above its full power operating temperature. Such tests would appear to be unnecessary as the present results extend the range of the Arrhenius dependence of the DHC velocity to sufficiently high temperature to be applicable for a Leak-Before-Break analysis for ACR pressure tubes for which the pressure tube outlet temperatures are expected to be about 330°C. Therefore, it is appropriate to use the 95% upper bound value of the current database for the axial DHC velocity as a conservative estimate in Leak-Before-Break analyses for ACR pressure tubes.

ACKNOWLEDGEMENTS

The authors would like to thank Wayne Ferris for hydriding the material, Kevin McCarthy and John Smeltzer for preparing the specimens, John Balfour for carrying out the experiments, and Craig Buchanan for performing metallographic analyses.

REFERENCES

1 Moan, G.D., Sagat, S., Ellis, P.J., Mistry, J.K., Richinson, P.J., Rodgers, D.K., and Coleman, C.E., "Leak-Before-Break in CANDU pressure tubes, recent advances," 1993 ASME Pressure Vessels and Piping Conference, Denver, Colorado, (1993).

2 Sagat, S., Coleman, C.E., Griffiths, M., and Wilkins, B.J.S., "The Effect of fluence and irradiation temperature on delayed hydride cracking in Zr-2.5Nb", Zirconium in the Nuclear Industry: Tenth International Symposium, ASTM STP 1245, A.M. Garde and E.R. Bradley, Eds., American Society for Testing and Materials, West Conshohocken, PA, (1994), pp. 35-61.

3 Sagat, S. and Puls, M.P., "Temperature Limit for Delayed Hydride Cracking in Zr-2.5Nb Alloys," In Proceedings of the17th SMiRT Conference, Prague, (2003).

4 Shi, S.Q. and Puls, M.P., "Criteria for fracture initiation at hydrides in zirconium alloys I. Sharp crack tip", J. Nucl. Mater., Vol. 208 (1994) pp. 232-242.

5 Shi, S.Q., Shek, G.K. and Puls, M.P., "Hydrogen concentration limit and critical temperatures for delayed hydride cracking in zirconium alloys", J. Nucl. Mater., Vol. 218 (1995) pp. 189-201.

6 Shek, G.K., Jovanovic, M.T., Seahra, H., Ma, Y., Li, D. and Eadie, R.L., "Hydride Morphology and striation formation during delayed hydride cracking in Zr-2.5%Nb", J. Nucl. Mater., Vol. 231 (1996) pp. 221-230.

7 Jovanovic, M.T., Shek, G.K., Seahra, H. and Eadie, R.L., "Metallographic and fractographic observations of hydrides during delayed hydride cracking in Zr-25% Nb Alloy", Materials Characterization, Vol. 40 (1998) pp. 15-25.

8 Shi, S.Q. and Puls, M.P., "Dependence of the threshold stress intensity factor on hydrogen concentration during delayed hydride cracking in zirconium alloys", J. Nucl. Mater., Vol. 218 (1994) pp. 30-36.

9 Puls, M.P., "Effects of crack tip stress states and Hydride-matrix interaction stresses on delayed hydride cracking", Metall. Trans., Vol. 21A (1990) pp. 2905-2917.

10 Pan, Z.L., Ritchie, I.G. and Puls, M.P., "The terminal solid solubility of hydrogen and deuterium in Zr-2.5Nb alloys", J. Nucl. Mater., Vol. 228 (1996) pp. 227-237.

11 Puls, M.P., "On the consequence of hydrogen supersaturation effects in Zr alloys to hydrogen ingress and delayed hydride cracking," J. Nucl. Mater., Vol. 165 (1989) pp.128-141.

Table 1 DHC velocity of irradiated material initially heated to 386℃, then cooled to test temperature

Specimen Identification	Sequence # **	Test Temperature (°C)	DHC Velocity (m/s)	K_I Initial (MPa m)	K_I Final (MPa m)	Calculated Average Plastic Zone Size (μm)	Measured Striation Spacing (μm)	Calculated Critical Hydride Fracture Length, L_c (μm)	Calculated* K_{IH} (MPa m)
1698_2	3	150	$7.75x10^{-9}$	22.4	27.2	95	---	4.8	5.6
1698_9	4	150	$1.05x10^{-8}$	26.6	31.2	197	---	4.8	5.6
1698_2	2	200	$3.61x10^{-8}$	19.3	23.4	89	14.3	6.6	6.2
1698_9	3	200	$4.48x10^{-8}$	22.2	26.5	116	---	6.6	6.2
1698_12	3	250	$2.12x10^{-7}$	29.1	36.7	445	---	9.4	6.9
1698_2	1	250	$1.38x10^{-7}$	16.6	20.3	85	13.5	9.4	6.9
1698_12	2	280	$4.26x10^{-7}$	25.2	30.9	360	13.8	11.9	7.4
1698_10	4	300	$5.09x10^{-7}$	24.9	28.6	351	---	14.3	7.9
1698_9	2	300	$4.81x10^{-7}$	18.7	22.2	132	21.1	14.3	7.9
1698_5	3	310	$5.16x10^{-7}$	22.4	27.2	270	---	15.8	8.2
1698_9	1	310	$6.77x10^{-7}$	17	21.1	121	17.0	15.8	8.2
1698_10	3	320	$6.12x10^{-7}$	20.9	25.9	253	26.7	17.6	8.5
1698_5	2	320	$5.93x10^{-7}$	19.6	23.6	214	21.1	17.6	8.5
1698_8	4	320	$5.70x10^{-7}$	27.0	31.4	452	22.9	17.6	8.5
1698_11	4	325	$8.7x10^{-7}$	25.4	31.0	432	22.0	18.7	8.7
1698_10	2	330	$1.77x10^{-7}$	18.4	20.9	142	35.2	19.8	8.9
1698_5	1	330	$4.21x10^{-7}$	17.3	19.9	127	40.0	19.8	8.9
1698_8	3	330	$5.71x10^{-7}$	21.3	26.0	269	30.8	19.8	8.9
1698_11	3	335	$7.90x10^{-7}$	20.1	25.3	255	28.6	21.1	9.1
1698_10	1	340	$1.27x10^{-7}$	17.1	18.8	125	---	22.6	9.3
1698_8	2	340	$2.00x10^{-7}$	17.8	20.9	145	30.8	22.6	9.3
1698_11	2	345	$2.02x10^{-7}$	17.4	20.6	144	---	24.2	9.6
1698_8	1	350	$2.92x10^{-8}$	17.2	17.9	125	---	26.1	9.9
1698_4	1	350	$4.00x10^{-9}$	15.9	15.7	101	81.0	26.1	9.9
1698_11	1	355	$2.29x10^{-8}$	17.4	18.0	131	---	28.3	10.2
1698_3	1	360	$1.04x10^{-9}$	17.8	17.2	131	90.3	30.9	10.6
1698_7	1	365	$3.40x10^{-11}$	15.0	14.8	98	---	33.9	11.0

* Using plastic zone normal stress $=0.738\ \sigma_y/(1-2\nu)$ and a temperature-dependent ν.

**Most specimens are subjected to multiple tests. Sequence number refers to the sequence of the test for the given specimen.

Table 2 KIH of irradiated material

Specimen Identification	Test Temperature (^{o}C)	Measured K_{IH} (MPa m)	Calculated * K_{IH} (MPa m)
1695_6B	130	6.8	5.4
1695_7A	130	6.4	5.4
1695_2A	240	7.4	6.7
1695_4B	240	8.0	6.7
1695_5A	240	7.1	6.7
1695_7B	240	7.3	6.7
1695_8A	240	7.6	6.7
1695_5	280	8.1	7.4
1695_1	300	9.4	7.9
1695_2B	310	8.4	8.2
1695_3B	310	8.3	8.2
1695_6	310	9.5	8.2
1695_2	320	15.5	8.5
1695_4A	320	9.0	8.5
1695_8B	330	12.3	8.9
1695_3	340	16.4	9.3

*Using plastic zone normal stress =0.738 $\sigma_y/(1-2\nu)$ and a temperature-dependent ν

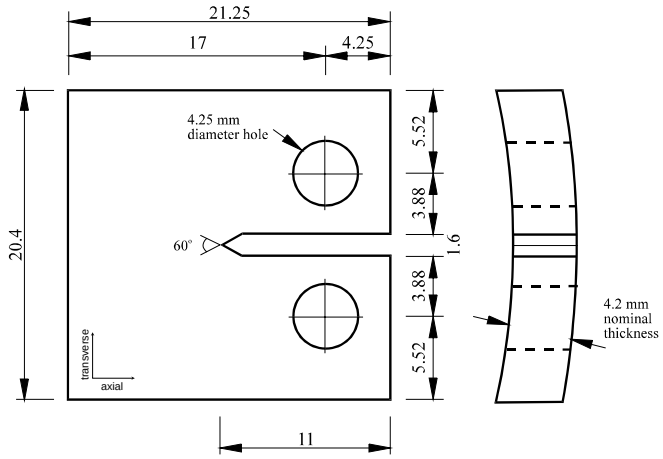

Figure 1 Schematic of CCT specimen for testing DHC velocity in axial direction (all dimensions in mm).

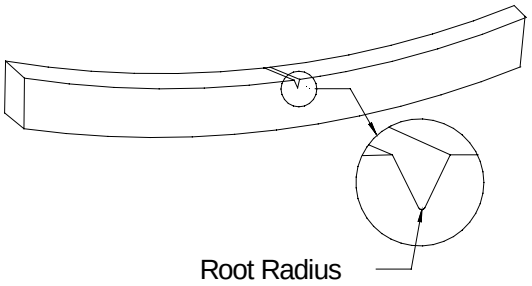

Specimen depth:	wall thickness of the pressure tube (~4.2 mm)
Specimen breadth:	3.2 mm
Specimen length;	19 or 38 mm
Notch depth:	0.5 mm
Notch:	45° included angle in the centre of the specimen length
Notch root radius:	broached with very sharp (<10 μm)

Figure 2 Schematic of CB specimen for testing KIH in radial direction.

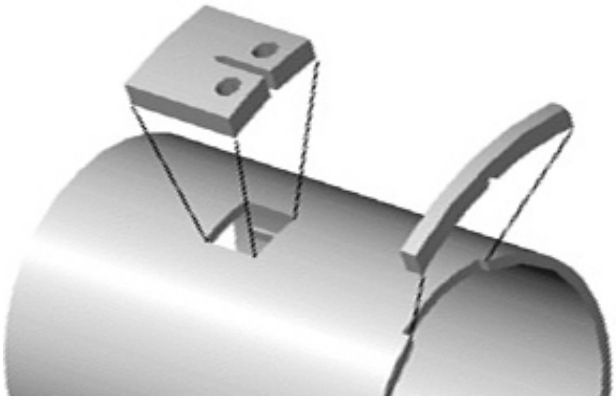

Figure 3 Schematic of CB and CCT specimen orientations in pressure tube.

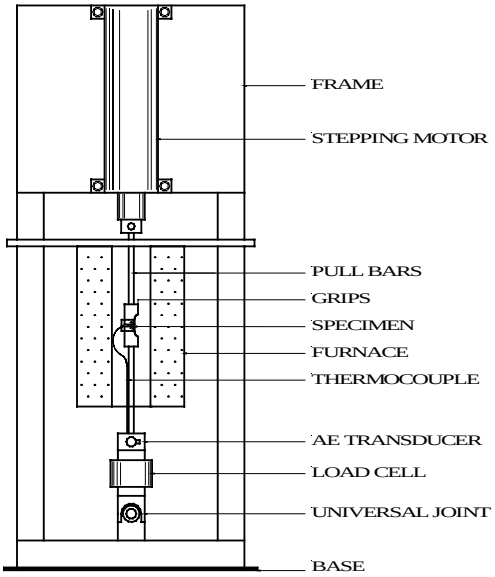

Figure 4 A schematic diagram of test apparatus for CCT specimens.

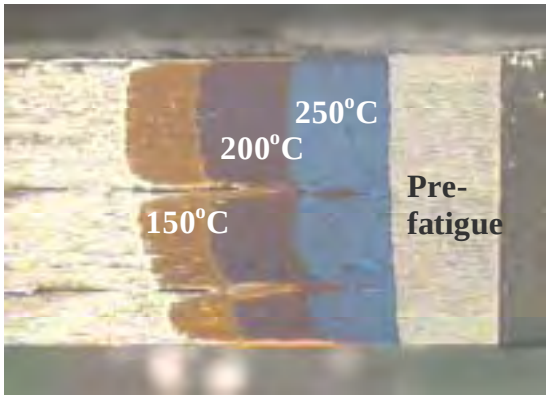

Figure 5 View of oxide-coloured crack zones in broken open specimen No. 1698_2.

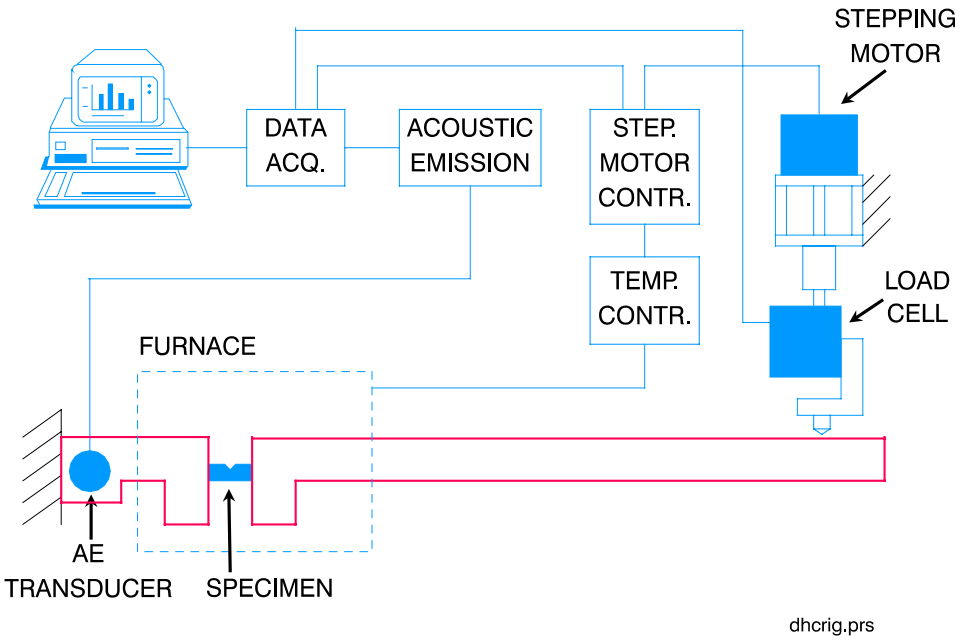

Figure 6 A schematic diagram of DHC test rig for CB specimens and control system.

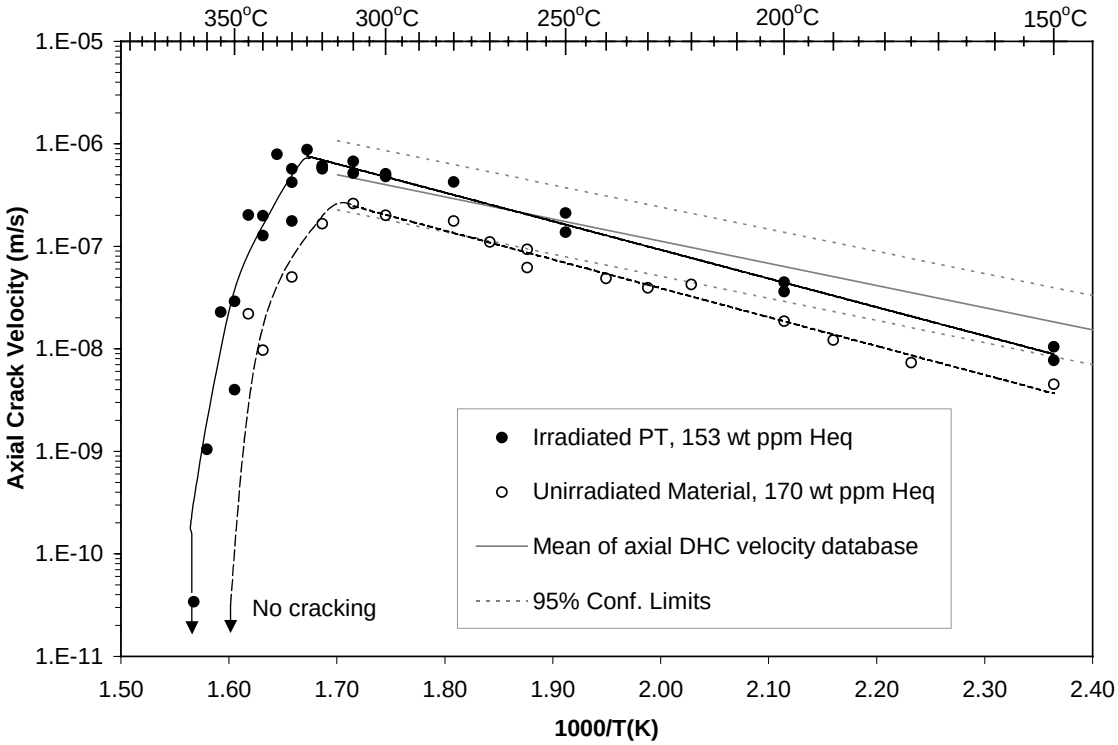

Figure 7 High-temperature axial crack velocity results for irradiated material.

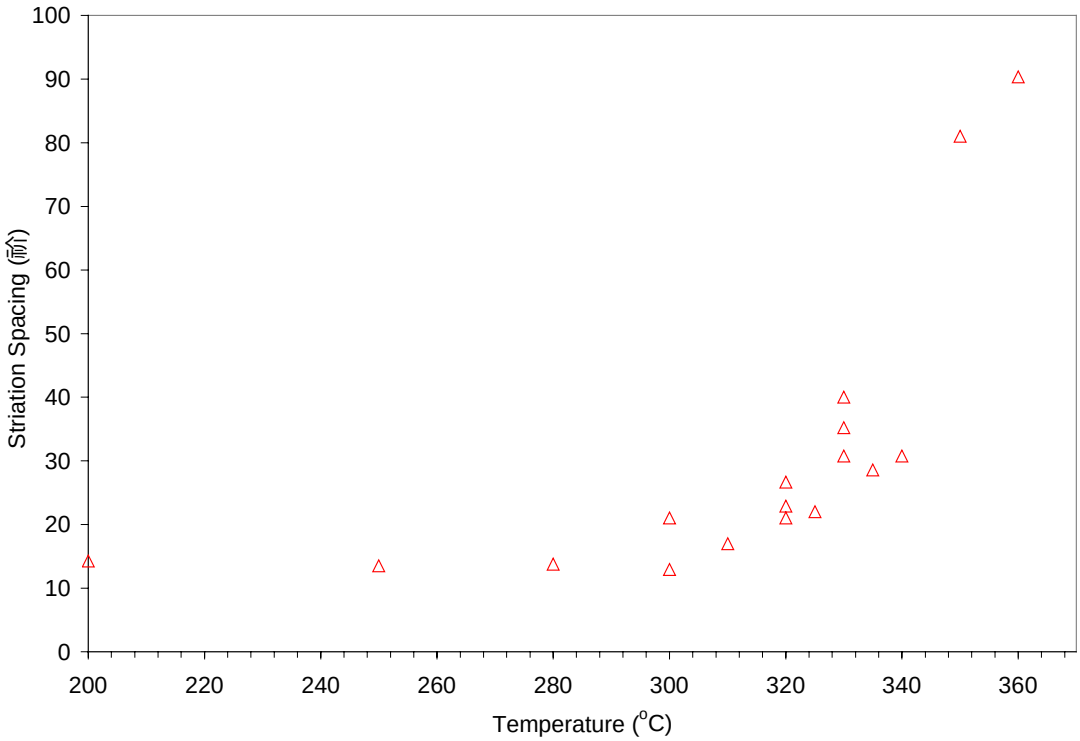

Figure 8 Average striation spacing in axial cracking direction from DHC crack for tests at different temperatures.

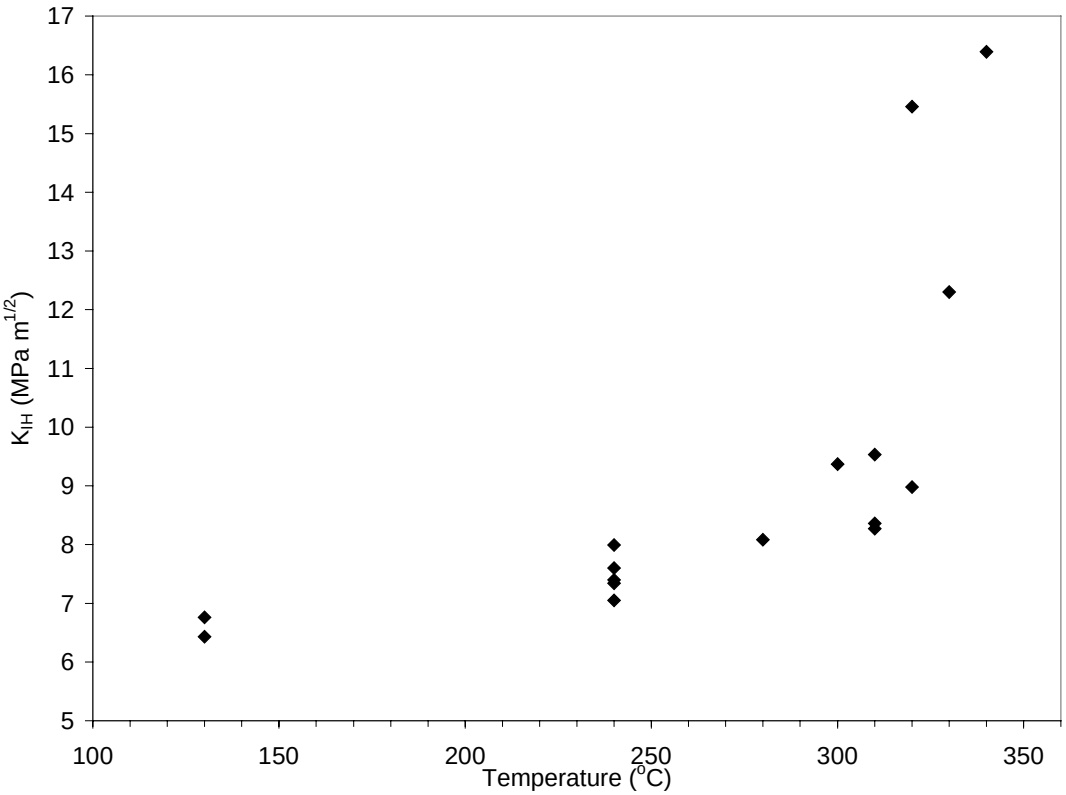

Figure 9 KIH from irradiated pressure tube with 153 wt ppm [Heq].

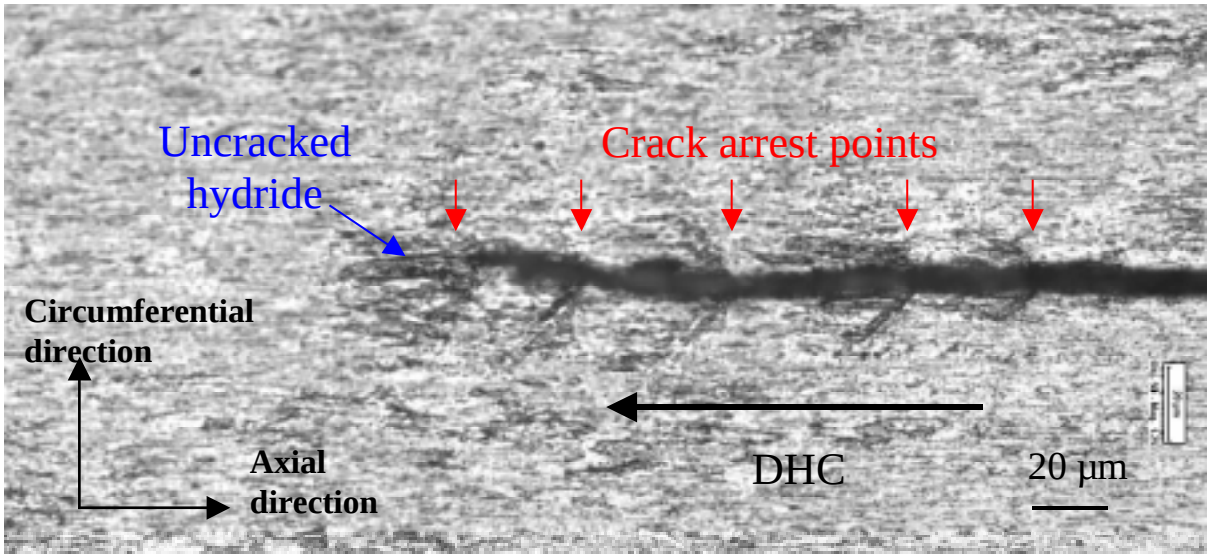

Figure 10 Arrest points of crack-tip during DHC at 360°C (Specimen No. 1698_3) . These are marked by hydrides at 45o at both sides of the crack (like "moustaches") produced by plasticity. The average crack arrest spacing is about 44 µm. An uncracked hydride of about 38 µm can be observed at the final crack tip. See also Fig. 11.

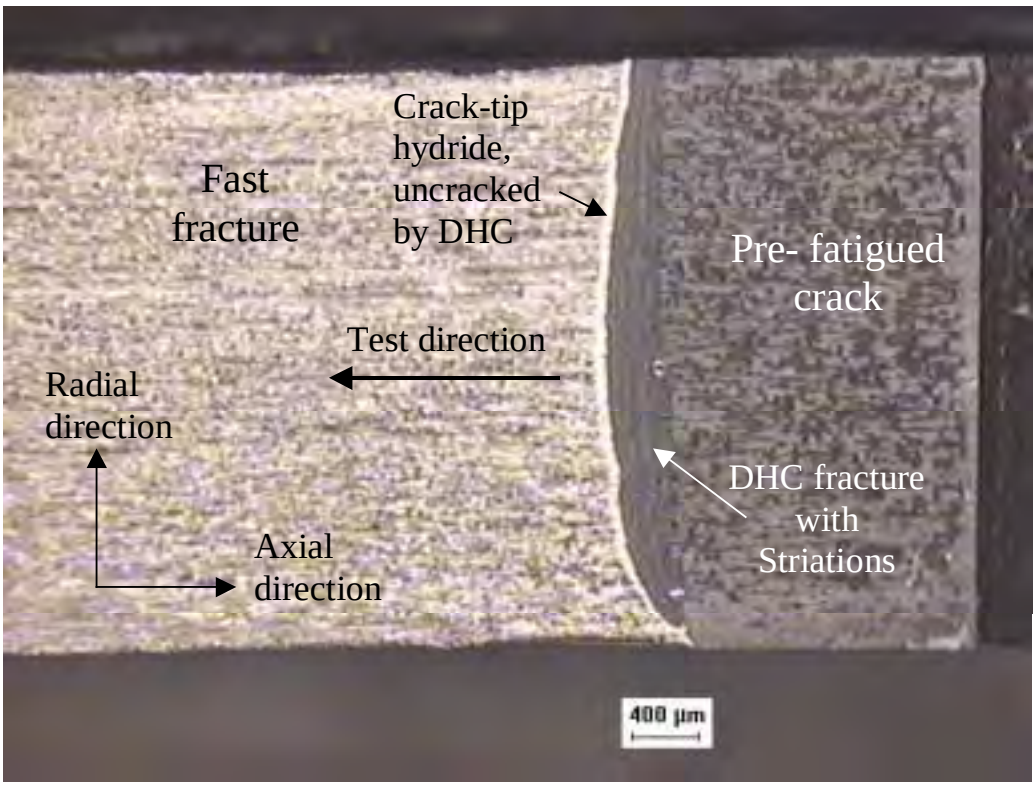

Figure 11 The broken open Specimen No. 1698_3 (Fig. 10) after metallographic examination. The metallographic surface of Fig. 10 corresponds to the upper edge of the specimen. The striation spacing at this edge is much less than that at the centre of the specimen. Here the striation spacing is about 90 µm (compared to 44 µm of crack arrest spacing in Fig. 10).